isvr Institute of Sound and Vibration Research

A Method for Estimating Sound Speed and the Void Fraction of Bubbles from Sub-Bottom Sonar Images of Gassy Seabeds

T.G. Leighton

ISVR Technical Report No 320

December 2007

University of Southampton

SCIENTIFIC PUBLICATIONS BY THE ISVR

Technical Reports are published to promote timely dissemination of research results by ISVR personnel. This medium permits more detailed presentation than is usually acceptable for scientific journals. Responsibility for both the content and any opinions expressed rests entirely with the author(s).

Technical Memoranda are produced to enable the early or preliminary release of information by ISVR personnel where such release is deemed to the appropriate. Information contained in these memoranda may be incomplete, or form part of a continuing programme; this should be borne in mind when using or quoting from these documents.

Contract Reports are produced to record the results of scientific work carried out for sponsors, under contract. The ISVR treats these reports as confidential to sponsors and does not make them available for general circulation. Individual sponsors may, however, authorize subsequent release of the material.

A Method for Estimating Sound Speed and the Void Fraction of Bubbles from Sub-bottom Sonar Images of Gassy Seabeds

T G Leighton

ISVR Technical Report No. 320

December 2007

UNIVERSITY OF SOUTHAMPTON

INSTITUTE OF SOUND AND VIBRATION RESEARCH

FLUID DYNAMICS AND ACOUSTICS GROUP

A Method for Estimating Sound Speed and the Void Fraction of Bubbles from Sub-bottom Sonar Images of Gassy Seabeds

by

T G Leighton

ISVR Technical Report No. 320

December 2007

Authorized for issue by
Professor R J Astley, Group Chairman

ACKNOWLEDGEMENTS

This work is funded by the Engineering and Physical Sciences Research Council, Grant number EP/D000580/1 (Principal Investigator: TG Leighton). The author is grateful to Justin Dix for providing the background data to figure 3 (water depth, and the density and sound speed of the bubble-free sediment) and to Gary Robb for useful comments on the manuscript.

CONTENTS

ABSTRACT

There is increasing interest in the effect of bubbles in gassy sediment. This is, first, because of the impact those bubbles have on the structural integrity and load-bearing capabilities of the sediment; second, because the presence of bubbles can be indicative of a range of biological, chemical or geophysical processes (such as the climatologically-important flux of methane from the seabed to the atmosphere); and third, because of the effect which the bubbles have on any acoustic systems used to characterise the sediment. For this reason, a range of methods have been investigated for their ability to estimate the bubble population in the seabed. Within such a range, there will a mix of advantages and limitation to given techniques. This report outlines a very basic method by which an observations which have already been taken for other purposes (sub-bottom profiles) may be subjected to a rapid analysis to obtain an estimate of the effect of bubbles on the sound speed in the sediment, and from there to provide a rapid preliminary estimate of the void fraction of bubbles present (assuming quasi-static bubble dynamics). This approach is not meant to compete with large-scale field trials which deploy specialist equipment to monitor gas bubbles in sediment, but rather to provide a method to exploit archived sub-bottom profiles, or to survey a large area rapidly with commercial equipment from a small vessel, in order to obtain an estimation of the local void fractions present, and their location and extent in three dimensions.

LIST OF FIGURES

Tables

1 Introduction

Marine sediments containing gas bubbles occur at many locations [*Judd and Hovland,* 1992; *Fleischer et al.*, 2001]. They are important, first, because of the impact those bubbles have on the structural integrity and load-bearing capabilities of the sediment [*Wheeler and Gardiner*, 1989; *Sills et al.*, 1991]; second, because the presence of bubbles can be indicative of a range of biological, chemical or geophysical processes (such as the climatologically-important flux of methane from the seabed to the atmosphere [*Judd*, 2003]); and third, because of the impact which the bubbles have on any acoustic systems used to characterise the sediment [*Robb et al.*, 2006, 2007a, 2007b; *Leighton et al.*, 2007a, 2007b].

When driven by an acoustic field, a gas bubble surrounded by a suitable host material acts as a nonlinear oscillator (which tends to linear dynamics at low pulsation amplitudes). It exhibits a pronounced breathing-mode resonance such that, when driven at frequencies much less than this resonance, its response is stiffness-controlled, and the presence of bubble reduces the sound speed (tending to quasi-static conditions at very low driving frequencies). When driven at frequencies much greater than resonance, the bubble's response is inertia-controlled, and the presence of bubbles tends to increase the sound speed, the effect decreasing with increasing frequency [*Leighton*, 1994].

Whilst there is a considerable body of work in the literature on the theory of acoustic propagation in marine sediments, the incorporation of gas bubbles into such theories is done with the inclusion of assumptions which severely limit the applicability of those models to practical gas-laden marine sediments. As a result, such theories are limited in terms of which components of the above behaviour they can describe [*Leighton et al.*, 2004]. The theories most frequently used include modified versions of the Biot-Stoll Theory [*Biot*, 1956a, 1956b; *Stoll*, 1974] and an approach developed by *Anderson and Hampton* [1980a, 1980b]. The Biot model assumes that the bubble does not affect the sediment structure (i.e. it only affects the pore fluid properties). Most manifestations of the Biot model assume quasi-static bubble responses [*Domenico*, 1976, 1977; *Andreassen et al.*, 1997; *Hawkins and Bedford*, 1992, *Gregory*, 1976; *Herskowitz et al.*, 2000; *Minshull et al.*, 1994; *Smeulders and Van Dongen*, 1997]. The assumption of quasi-static gas dynamics limits the applicability of the resulting theory to cases where the frequency of insonification is very much less than the resonances of any bubbles present. It also eliminates from the model all bubble resonance effects, which often of are overwhelming practical importance when marine bubble populations are insonified. This limitation becomes more severe as gas-laden marine sediments are probed with ever-increasing frequencies [*Leighton et al.*, 2007a, 2007b].

Some versions of the Biot model include a simple harmonic oscillator term for the compressibility of the fluid, which incorporates the inertia, stiffness and damping terms relevant to the bubbles [*Biot,* 1962; *Stoll and Bautista,* 1998]. The acoustic theory of *Anderson and Hampton* [1980a, 1980b] similarly assumes that only linear, steady state bubble pulsations occur. As a result, neither class of theory is applicable to the propagation of fields which are sufficiently high amplitude: the ubiquitous assumption of linear bubble pulsations becomes increasingly questionable as acoustic fields of greater amplitudes are used to overcome the high attenuations, and the resulting poor-signal-to-noise ratios, that are often encountered in marine sediments. Furthermore the assumption of monochromatic steady-state bubble dynamics is inconsistent with the use of short acoustic pulses to obtain range resolution.

A further complication which limits the applicability of models of the dynamics of gas bubbles in sediments, is the bubbles may not be spherical at all times. It is well-known that there are classes of bubbles in sediment which do not behave in this way (e.g. those which bear a closer resemblance of 'slabs of gas' and 'gas-filled cracks', than they do to gas-filled spheres [*Hill et al.*, 1992; *Anderson et al.*, 1998; *Reed et al.*, 2005]).

This report outlines the use of a very simple theory, which models the bubbles as non-interacting linear oscillators. An 'effective medium approach' is used to generate a form of Wood's equation. It then uses that theory to demonstrate a simple method of estimating the bubble void fraction, which is valid in conditions where the bubbles are insonified at frequencies much less than the general resonance of the bubble population.

2 Effective medium model

Consider a volume V_{eff} of seabed which is considered to be an effective medium to which parameters pertinent to the sound speed can be assigned. It is considered to consist of two constituent effective medium: gas, and 'non-gassy material' (water plus solid). The volume V_{eff} contains a volume V_{s} of non-gassy material, and a volume V_{g} of gas (distributed amongst a population of bubbles). Conservation of volume gives:

$$V_{\text{eff}} = V_{\text{g}} + V_{\text{s}} . \qquad (1)$$

Mass conservation is simply expressed by multiplication of the volumes with the respective densities (of effective medium, ρ_{eff}; and of gas, ρ_{g}; and where ρ_{s} is the spatially-averaged density of all the non-gassy component). Mass conservation gives:

$$\rho_{\text{eff}} V_{\text{eff}} = \rho_{\text{g}} V_{\text{g}} + \rho_{\text{s}} V_{\text{s}} . \qquad (2)$$

Under the assumption that each of the three media (gas, non-gassy media, and the effective medium of the seabed) conserves mass separately, the differential of Eq. (2) with respect to the applied pressure P is, of course, zero. In an infinite body of either water or gas that contains no dissipation, sound speeds (c_{g} and c_{s}, respectively) may be defined according to:

$$c_{\varepsilon}^2 = \frac{B_{\varepsilon}}{\rho_{\varepsilon}} = \left(\frac{\partial P(\rho, S)}{\partial \rho} \right)_{\varepsilon} \quad (\varepsilon = \text{s,g}), \qquad (3)$$

where S is the entropy and the subscript ε can refer to application to non-gassy medium (s) or the gas (g). Similarly, differentiation of Eq. (1) with respect to the applied pressure gives, with Eq. (3), the relationship between the bulk moduli of the effective medium (B_{eff}) and the gas (B_{g}), and the bulk modulus of the non-gassy material (B_{s}):

$$\frac{1}{B_{\text{eff}}} = \frac{V_{\text{g}}}{V_{\text{eff}}} \frac{1}{B_{\text{g}}} + \frac{V_{\text{s}}}{V_{\text{eff}}} \frac{1}{B_{\text{s}}} = \beta \frac{1}{B_{\text{g}}} + (1-\beta) \frac{1}{B_{\text{s}}} , \qquad (4)$$

where $\beta = V_{\text{g}} / V_{\text{eff}}$ is the void fraction. Let us define a function ζ_{eff} (which is not an inherent property of the bubble cloud in the thermodynamic sense), equal to the root of the ratio of the bulk modulus of the bubbly cloud to its density [*Leighton et al.* 2004], which with Eq. (4) gives:

$$\begin{aligned} \zeta_{\text{eff}} &= \sqrt{\frac{B_{\text{eff}}}{\rho_{\text{eff}}}} = \sqrt{\left(\frac{V_{\text{eff}}}{\rho_{\text{g}} V_{\text{g}} + \rho_{\text{s}} V_{\text{s}}} \right) \Big/ \left(\frac{V_{\text{g}}}{V_{\text{eff}} B_{\text{g}}} + \frac{V_{\text{s}}}{V_{\text{eff}} B_{\text{s}}} \right)} \\ &= \sqrt{\left(\frac{1}{\rho_{\text{g}} \beta + \rho_{s} (1-\beta)} \right) \Big/ \left(\frac{\beta}{B_{\text{g}}} + \frac{1-\beta}{B_{\text{s}}} \right)} \\ &= \left(\rho_{\text{g}} \beta + \rho_{\text{s}} (1-\beta) \right)^{-1/2} \left(\frac{\beta}{B_{\text{g}}} + \frac{1-\beta}{B_{\text{s}}} \right)^{-1/2} \end{aligned} \qquad (5)$$

Equation (5) for the sound speed in a two-phase medium is also known as Wood's equation (Wood 1964), which applies to a suspension (such as mineral particles in water) or to any medium lacking rigidity, in terms of weighted means of the densities and the compressibilities of the two constituents of the material. Clearly it is only a limited model of the real situation in gassy sediments, but it serves for the simple method of interpretation which will be used in this paper.

Assuming that the volume of gas is much less than the volume of non-gassy component, equation (5) simplifies through binomial expansion as follows:

$$\zeta_{\text{eff}} \approx \left(\frac{1}{c_{\text{s}}^2} + \frac{\beta B_{\text{s}}}{c_{\text{s}}^2 B_{\text{g}}} \right)^{-\frac{1}{2}} \qquad (6)$$

using (3), which through binomial expansion reduces to

$$\zeta_{\text{eff}} \approx c_{\text{s}} \left(1 - \frac{\beta B_{\text{s}}}{2 B_{\text{g}}} \right) . \qquad (7)$$

Furthermore from (3),

$$c_{\text{s}}^2 = B_{\text{s}} / \rho_{\text{s}} , \qquad (8)$$

and

$$B_{\text{g}} = -V_{\text{g}} \frac{\partial P}{\partial V_{\text{g}}} = -\frac{\partial P}{3 \partial R / R} \qquad (9)$$

Because the phase of the oscillation depends on the bubble equilibrium size and the insonifying conditions, the gradient of $\partial R / \partial P$ is a function of the bubble size, for given insonification conditions [*Leighton*, 2004; *Leighton et al.*, 2004]. The general case will therefore require that ζ_{eff} in (7) be evaluated through an integration over the bubble size distribution. For the simple purposes of the inversion required in this report, the inversion will be simplified through the use of quasi-static assumptions.

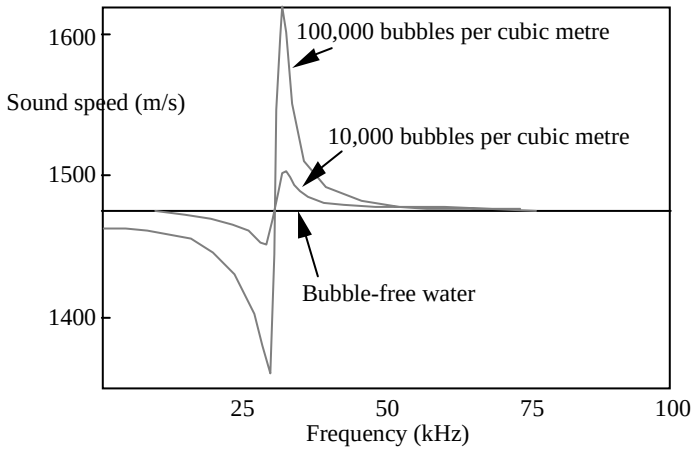

Figure 1. Schematic of the effect on sound speed of various monodisperse bubble populations of air in water (all bubbles are assumed to have an equilibrium bubble radius of 0.1 mm). This schematic is generated through qualitative consideration of the form of equation (9), assuming that all the non-gassy medium contains only water at 1 atmosphere static pressure.

The net effect of this can be seen in Figure 1. In quasi-static conditions (near DC), bubbles are more compressible than water, and the effect on compressibility is greater than the effect on

the density in determining the sound speed. At DC, a positive pressure causes a decrease in bubble volume, so that $\partial R / \partial P$ in equation (9) is negative, causing a decrease in sound speed. This effect increases as the bubble size approaches resonance. In the figure this occurs around 30 kHz. However like any oscillator the bubbles undergo a phase change of Pi as the frequency increases through resonance (taking them from a stiffness-controlled regime to an inertia-controlled regime).

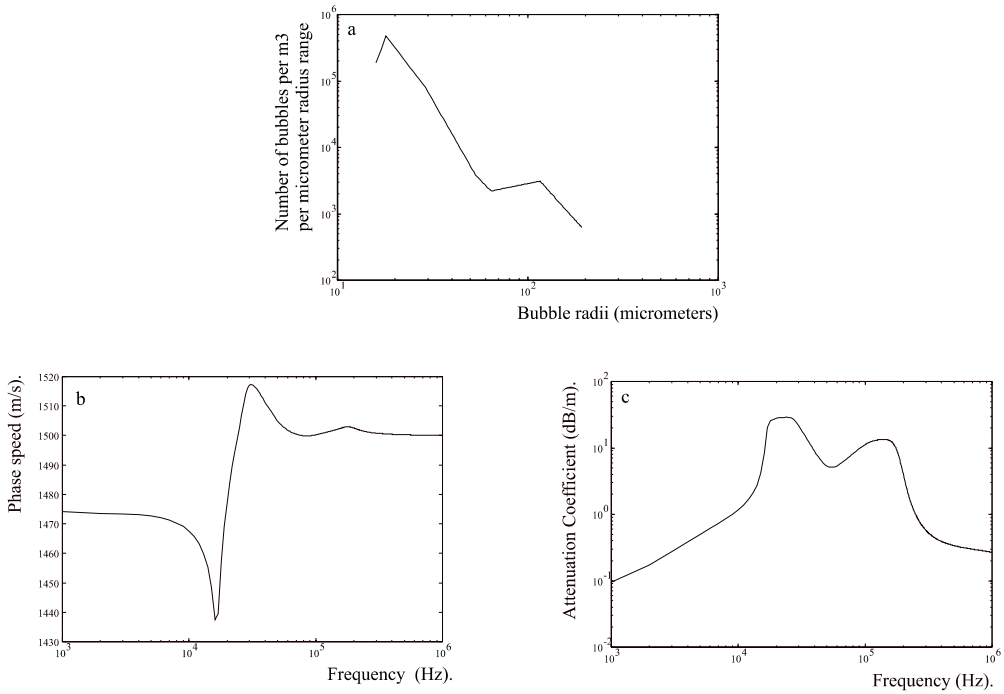

Figure 2. (a) The measured bubble size distribution found in the ocean [*Phelps and Leighton* 1998], from which the author (and student SD Meers) calculated (b) the phase speed and (b) the extra absorption which the addition of bubbles generates.

In the inertia-controlled regime, the bubbles are expanding during the compressive half-cycle of the acoustic pulse, and so $\partial R / \partial P$ in equation (9) is positive, causing an increase in sound speed. At the highest frequencies the acoustic cycle changes from compression to rarefaction at a rate so much faster than the response time of the bubble (approximately of the order of the period of its natural frequency) that the bubble pulsation is very low amplitude, and the effect of the bubbles on sound speed is minimal.

Whilst the above calculations were for monodisperse bubble populations (where all bubbles have roughly the same size), similar effects can be seen in polydisperse bubble populations (containing a wide range of bubble sizes). Consider the figure 2. Part (a) shows a bubble size distribution, measured in the oceanic water column, along with the associated sound speed (part (b)) and the component of attenuation for which bubbles are responsible (part (c)). Although a wide range of bubble sizes are present (from at least microns to

millimetres) in the ocean, the population as a whole tends to impart to the ocean characteristics such that, for frequencies below about 20 kHz, the bubbles reduce the sound speed to less than that of bubble-free water (~1480 m s^{-1}), However, for frequencies above about 40 kHz, the bubbles tend to increase the sound speed (part (b)), returning to the sound speed of bubble-free water at the highest frequencies. The magnitude of the change to sound speed increases the closer the insonifying frequency is to the critical 30-50 kHz range. The additional attenuation caused by bubbles (over and above that which occurs in bubble-free water) also peaks in this range (part (c)).

Given these considerations, therefore, let us return to consideration of how the bubble population can have attributed to it a series of assumptions simple enough to allow a ready inversion, to obtain an estimation of the void fraction from the bubble-induced sound speed perturbation. If the insonification frequency is sufficiently less than the main resonance of the bubbles present (noting from Figure 2 that even the broad distribution of Figure 2(a) exhibits a main resonance in Figure 2(b)), then $\partial R / \partial P$ does not vary greatly between the various bubbles in the population [*Leighton*, 2004; *Leighton et al.*, 2004]. In the linear limit of small-amplitude bubble pulsations we have:

$$\frac{dR}{dP} = \frac{-1}{R_0 \rho_s ((\omega_0^2 - \omega^2) + 2\mathrm{i}\beta_{\mathrm{tot}}\omega)}, \qquad (10)$$

where β_{tot} is a damping parameter of dimensions time^{-1}, and ω_0 is the circular pulsation resonance frequency. [*Leighton et al.* 2004]. If all the bubbles in the population were the same size, of radius R_0, and undergoing linear pulsations, then substitution of (8), (9) and (10) into (7) would give:

$$\zeta_{\mathrm{eff}} \approx c_s \left(1 + \frac{3\beta B_s}{2R}\frac{\partial R}{\partial P}\right) \approx c_s \left(1 - \frac{3\beta}{2R_0^2}\frac{B_s/\rho_s}{(\omega_0^2 - \omega^2) + 2\mathrm{i}\beta_{\mathrm{tot}}\omega}\right), \qquad (11)$$

which, when the frequency of insonification tends to much less than the resonance of the bubbles present[1], tends to

$$\zeta_{\mathrm{eff}} \approx c_s \left(1 - \frac{3\beta c_s^2}{2R_0^2\omega_0^2}\right), \qquad (\omega << \omega_0) \qquad (12)$$

.

If the bubble resonance frequency can be assumed to resemble the equivalent Minnaert frequency, i.e.

$$\omega_0^2 \approx \frac{3\kappa p_0}{R_0^2 \rho_s}, \qquad (13)$$

[1] The insonification frequency of the chirp used to obtain Figure 3 ranged from 2 kHz to 8 kHz in a linear sweep of 32 ms duration, which therefore will mean that, whilst it is certainly possible that this condition was met for most of the bubbles present, it is unlikely that it was met for all.

where p_0 is the static pressure at the position of the bubble, ρ_s is the equilibrium density in the effective medium, and κ is the polytropic index of the gas within the bubbles, then (12) reduces to:

$$\zeta_{\text{eff}} \approx c_s \left(1 - \frac{\beta c_s^2 \rho_s}{2\kappa p_0} \right) \qquad (\omega << \omega_0) \qquad (14)$$

3. Use of the effective medium model to interpret sub-bottom profiles

Consider Figure 3. It is a chirp sonar image, showing a cross-section of the seabed (maximum penetration approximately 20 m) in Strangford Lough, Northern Ireland [Lenham *et al*., 1998]. The dark line, which is usually 8-10 m from the top of the frame, indicates the sea floor. Hence the labelled features are beneath the seabed. These include shallow gas deposits in the underwater sediment. The sonar cannot penetrate these, as the majority of the sound is scattered from the gas bubbles. As a result, very little information is obtained from beneath the gas layers. The range is calculated by assuming that the sound speed in the water column velocity was 1480 ms^{-1}, and for this Strangford section sediment package the sound speed was 1600 ms^{-1}.

However before the geological layering features on either side of the gas pockets become obscured, they appear to dip to greater depths. If it is assumed that in fact these features in actual fact remain at roughly constant depth, then this perceived dipping could be attributed to a reduction in the sound speed.

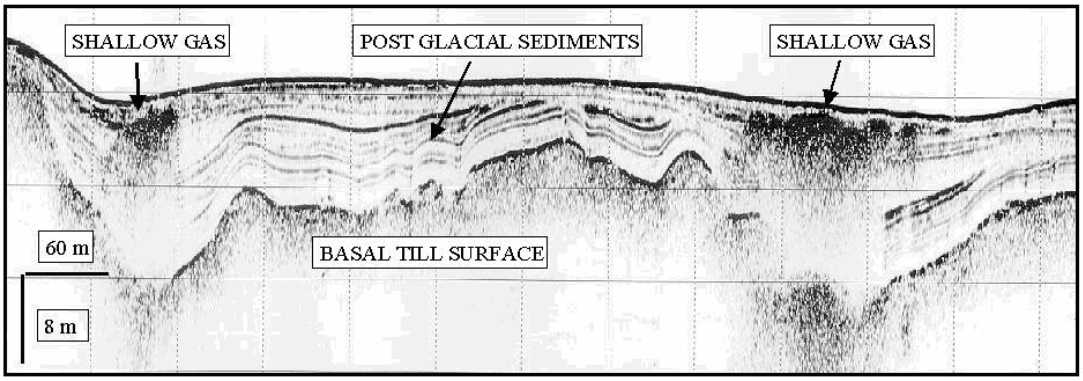

Figure 3. A chirp sonar image, showing a cross-section of the seabed (maximum penetration approximately 20 m) in Strangford Lough, Northern Ireland. Reproduced by permission of Southampton Oceanography Centre (J.S. Lenham, J.K. Dix and J. Bull). The depth of the water was estimated to be 15.5 m.

Assume a layer feature is at depth d_s below the seabed, which is itself at a depth d_w below the sonar source (which is usually close to the sea/air interface). The sound speed in the gas-free regions of the seabed is c_s, and in the water column it is c_w. From Figure 4, the two-way travel time for an echo from the layer feature is:

$$t_2 = 2(d_w / c_w + d_s / c_s) \quad (15)$$

The terms d_w and c_w can be assigned values with relative ease (a procedures common in bottom profilers), since the two-way travel time for an echo from the top of the sediment (Figure 4) is:

$$t_1 = 2d_w / c_w \quad (16)$$

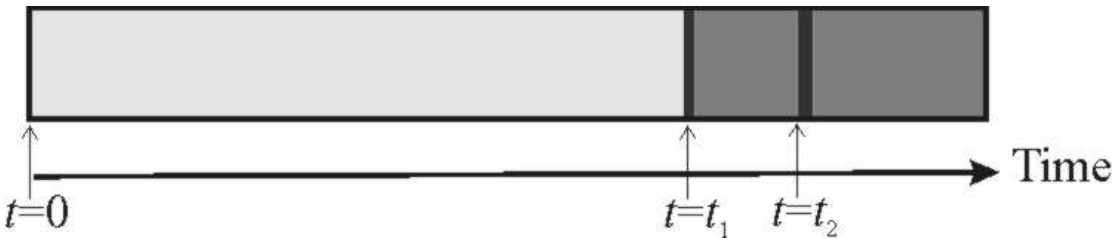

Figure 4. Schematic representation showing power in returned signal (the darker grey, the more power) as a function of time (the datum corresponding to transmission of the pulse).

In order to establish the depth below the seabed at which a strongly reflecting layer generates an echo, the time of interest is that delay from the echo which corresponds to the top of the seabed, to the echo from some region at point, i.e.

$$t_2 - t_1 = 2d_s / c_s \quad (17)$$

such that the depth of that feature below the seabed is

$$d_s = c_s(t_2 - t_1) / 2 \quad (18)$$

Now imagine that the seabed contains a population which reduces the sound speed in the seabed from c_s to c_{eff}. The two-way travel time from the monostatic source to that reflecting layer is now:

$$t_3 = 2(d_w / c_w + d_s / c_{eff}) \quad (19)$$

and the delay between the echo from the top of the seabed, and the echo from the layer, arriving back at the position of the source is:

$$t_3 - t_1 = 2d_s / c_{\text{eff}} \quad (20)$$

Therefore the perceived depth of that layer below the seabed will now be:

$$d_{s2} = c_s(t_3 - t_1)/2 \quad (21)$$

Therefore the perceived change in depth of that later is:

$$d_{s2} - d_s = c_s(t_3 - t_1)/2 - c_s(t_2 - t_1)/2 = c_s d_s / c_{\text{eff}} - d_s \quad (22)$$

The sound speed change in the gassy sediment can therefore be calculated from the perceived depth change to be:

$$c_{\text{eff}} = c_s \left(1 + \frac{d_{s2} - d_s}{d_s} \right)^{-1} = c_s \frac{d_s}{d_{s2}} \quad (23)$$

Equation (23) indicates, for example, that if one were monitoring a large-scale gas blanket, then the depth of the perceived top of that blanket may be inaccurately calculated as being deeper than it is in reality, because of the presence of a more sparse bubble population at shallower depths which reduce the sound speed, but whose presence is overwhelmed in the sonar profile by the scatter from the top of the dense gas blanket. This effect could be tested by sweeping the frequency to test whether the perceived depth of the top of the gas blanket is frequency dependent, since at some frequencies it is possible for bubbles to increase the sound speed and so make this feature appear more shallow than it truly is (an event which would be valuable in estimate the bubble size distribution.

This paper utilises a different scenario, where the image includes the region between the edge of a gas layer and a bubble-free region of sediment. The approach provides a quick first-order technique, but the simplicity of its use is offset by limitations. The assumption of quasi-static bubble dynamics may be violated if the bubbles are sufficiently large or the insonification frequencies are sufficiently high. The bubbles are furthermore assumed to be spherical and bubble-bubble interactions are neglected. Any bubble-mediated changes in the sound speed profile are assumed to occur uniformly along a vertical line in the sediment: changes in this perturbation occur only in the horizontal. This will not be a realistic assumption if the gas populations varies in the vertical direction (as is almost certain) as well as the horizontal direction, along lengthscales of an acoustic wavelength or greater. The technique can of course be adapted to account for vertical variations in the bubble population through use of a varying sound speed along any vertical, although at the cost of adopting assumed characteristics for that variation.

4 Results

Considering the labels on Figure 5, whereby a sequence of points on the plot are indicated with labelled arrows. From the reasoning given earlier in this report, it is assumed that, at the points labelled B1, C1, D1, E1, F1 and G1, the presence has gas has made the perceived depth of layer 1 greater than the actual depth; and at the points labelled B2, C2, D2, E2, F2 and G2, the presence has gas has made the perceived depth of layer 2 greater than the actual depth.

From this hypothesis, the problem scenario is as follows. It is assumed that the sediment at the line joining A1 to A2 contains no bubbles, a not unreasonable assumption given the near-horizontal nature of both of the layer ('1' and '2') at these locations. It is further assumed that the layer labelled A1, B1, C1, D1, E1, F1, G1 is in reality at a constant depth (indicated by the position of 'A1') below the top of the seabed, but that the perceived dipping of this layer is caused by a reduction in sound speed in the sediment as a result of the presence of bubbles. Comparing the depth of 'A1' to each in turn of B1, C1, D1, E1, F1, G1 allows values of d_s / d_{s2} to be calculated for the location of each lettered label (Table 1). Similarly, it is assumed that the layer labelled A2, B2, C2, D, E2, F2, G2 is in reality at a constant depth (indicated by the position of 'A2') below the top of the seabed, but that the perceived dipping of this layer is caused by a reduction in sound speed in the sediment as a result of the presence of bubbles. Again, comparing the depth of 'A2' to each in turn of B2, C2, D2, E2, F2, G2 allows values of d_s / d_{s2} to be calculated for the location of each lettered label (Table 1). This then allows the estimated speed in the gassy sediment at that horizontal coordinate to be calculated (Table 1) through $c_{\text{eff}} = c_s d_s / d_{s2}$ (equation (24)). The results are shown in Figure 6. If the assumption (section 3) that the perturbation in sound speed is constant for any given horizontal coordinate were not to be true, the values of sound speed in series 1 for a particular letter would differ from that estimated in series 2 for the same letter (see the Appendix).

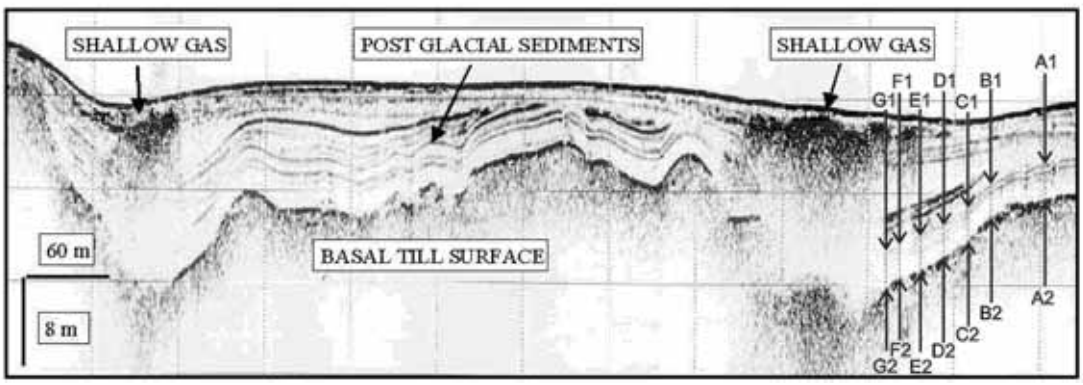

Figure 5. Reproduction of Figure 3 with location labels added (see text for details).

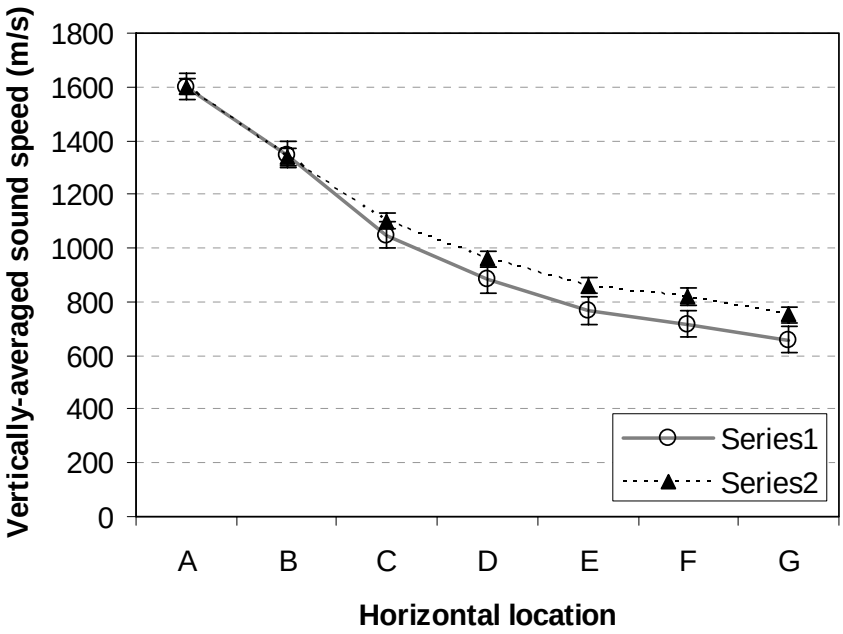

Figure 6. The estimated sound speed at the locations labelled on Figure 5. 'Series1' refers to the sound speed averaged between the top of the seabed and layer 1 (assumed to have a constant depth of 5.1 m). 'Series2' refers to the void fraction vertically-averaged between the top of the seabed and layer 2 (assumed to have a constant depth of 7.4 m).

Figure 6 shows that for the uncertainties associated with this data, it is not possible to prove such a violation of this assumption. As the Appendix shows, fact that the spacing between the two layers '1' and '2' in Figure 5 is expanded in proportion to the increase in depth, suggests that the gas layer extends from the surface to at least as deep as layer 2. The Appendix shows that, if the gas layer extended simply to as deep as layer 1, but the sediment were gas-less between layer 1 and 2, then the spacing between layers 1 and 2 would remain constant, although both would dip down to greater depths in the seabed as a result of the change in sound speed which occurs between the top of the seabed and layer 1.

Having estimated the sound speed at any particular horizontal coordinate, equation (14) can be rearranged to estimate the void fraction at that coordinate:

$$\beta \approx \frac{2\kappa p_0}{c_s^2 \rho_s}\left(1 - \frac{c_{\text{eff}}}{c_s}\right) \qquad (\omega << \omega_0) \qquad (24)$$

These void fractions can now be calculated, and will be done so to obtain estimates of the vertically-averaged void fraction between the top of the seabed and each of the layers (1 and 2) in turn.

At the time the measurements of Figure 3 were taken, techniques for measuring the density and sound speed in the sediment were not as advanced as they are today. The value

for the density of the saturated gas-free sediment will be used for ρ_s, although clearly with new data it would be better to measure ρ_s directly, particularly when the void fraction is high. A value of ρ_s =2300 kg m^{-3} for the silts and clays which are typical of the area was taken as a first estimate, suitable for this preliminary analysis [*Richardson & Briggs*, 1993].

The atmospheric pressure is taken to be 103 kPa (the data were recorded in the last few days in May 1997). The hydrostatic head of the 15.5 m water column would add to this a further 152 kPa contribution to the static pressure. Assuming (from the above discussion) a density of ρ_s =2300 kg m^{-3} kg m^{-3} for the sediment/water mixture found beneath the seabed, the contribution of the sediment to the static pressure at the bubble is estimated to be $\rho_s g h_1 \approx 115$ kPa at layer 1 (which is assumed to be at depth h_1 =5.1 m below the top of the seabed) and $\rho_0 g h_2 \approx 167$ kPa at layer 1 (which is assumed to be at depth h_2 =7.4 m below the top of the seabed) where g is the acceleration due to gravity (Table 1).

Since the inversions will be undertaken to obtain the vertically averaged void fraction between the top of the seabed and each layer in turn, the hydrostatic pressure to use will be that found half-way between the top of the seabed and the respective layer. Therefore the value used for p_0 when estimating the average void fraction between the top of the seabed and layer 1, will be (103 + 152 + 115/2) = 312.5 kPa. Similarly the value used for p_0 when estimating the average void fraction between the top of the seabed and layer 2, will be (103 + 152 + 167/2) = 338.5 kPa.

The sound speed c_s is taken from the gas-free measurement in Figure 6, which naturally reflects the value of the 1600 ms^{-1} sound speed which had been assumed for these frequencies for gas-free sediment used in converting the time series of the echo into Figure 3. The polytropic index is assumed to be κ =1.3, a value typical for bubbles containing the gas methane which are assumed to pulsate adiabatically.

The resulting void fractions are calculated in Table 1 for the coordinate in question, and plotted on Figure 7. The error bars in Figure 6 have not been translated onto Figure 7 because the assumptions in the sediment parameters introduce an unknown uncertainty.

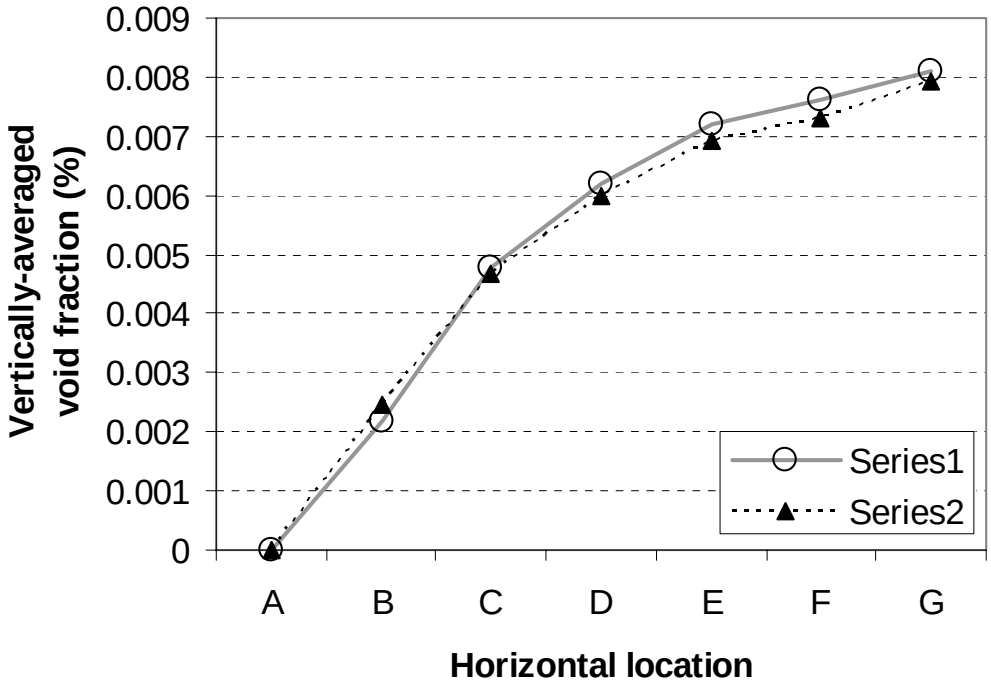

Figure 7. The estimated void at the locations labelled on Figure 5. 'Series1' refers to the void fraction vertically-averaged between the top of the seabed and layer 1 (assumed to have a constant depth of 5.1 m). 'Series2' refers to the void fraction vertically-averaged between the top of the seabed and layer 2 (assumed to have a constant depth of 7.4 m).

Horizontal location	Perceived depth of layer 1 (m)	Perceived depth of layer 2 (m)	Average sound speed between top of seabed and layer 1 (m/s)	Average sound speed between top of seabed and layer 2 (m/s)	Average void fraction between top of seabed and layer 1 (%)	Average void fraction between top of seabed and layer 2 (%)
A	5.1	7.4	1600	1600	0	0
B	6.0	8.9	1348	1338	0.0022	0.0024
C	7.7	10.8	1048	1100	0.0048	0.0047
D	9.2	12.4	882	959	0.0061	0.0060
E	10.6	13.8	767	859	0.0071	0.0069
F	11.3	14.5	716	819	0.0076	0.0073
G	12.3	15.8	659	752	0.0081	0.0079

Table 1. Estimated parameters for locations A to G in layer 1 and layer 2.

5 Conclusions

This report outlined a very simple scheme for assessing the sound speed perturbation induced by bubbles in the seabed, and for estimating the void fraction and extent of the bubble layers (in terms of its penetration depth into the seabed and its horizontal extent in the profile) using that scheme. If there is a location in an image where it is geologically reasonable and accurate to make the assumption that two layers should be at constant depth (or, if not, that the slope is known and constant from other data), then the vertically-averaged sound speed perturbation and bubble void fraction between those two layers can be estimated. With sufficient layers the seabed may be divided into vertically stacked layers, and the void fraction in each can be estimated, since the sound speed perturbation is simple the ratio of the actual separation of those layers to the perceived separation. As such, given sufficient layers, the profile of sound speed perturbations can be determined 'at a glance', as can its horizontal variation. The principle of the approach can be extent to three-dimensional profiles [*Bull et al.,* 2005a, 2005b; *Gutowski et al.,* 2008].

The simplicity of the scheme is bought at a price, in terms of the wide ranging assumptions that are made about the bubble and sediment. Most of those assumptions will be violated to a greater or lesser extent by the environmental and insonification conditions. Nevertheless, the ease with which first-order environmental data can be gained at little extra effort using existing technology and through examination of historical records of sub-bottom profiles, offers the possibility of making rapid progress rapidly. This is significant given:

(i) the usual interpretation when gas pockets of the sort shown in Figure 4 are visible in a sub-bottom profile is that, other than indicating the presence and location[2] of the pocket, that the presence of gas so disrupts the sub-bottom profile that it severely hinders the ability to analyse it at the location of the gas pocket;

(ii) the complexity of the acoustical interactions generated by gas pockets in sediment means that most experimental measurements of these require very complex equipment (including difference frequency sonars and CT scanners etc.) [*Wilkens and Richardson,* 1998; *Anderson et al.,* 1998; *Boudreau et al.,* 2005; *Ostrovsky et al.,* 2005]).

This study is of course in no way intended to complete with the innovative and large-scale field trials designed to measure at-sea bubble population in sediments. Rather it is a method of exploring the value of retrospectively analysing past sub-bottom profiles, and

[2] Note furthermore that the extent of the gas, as indicated by the void fractions shown in Figure 7, is much greater than the extent of the shadows in Figure 4 which, by visual inspection, one might consider to be the location and extent of the gas pocket.

asking what might be determined from routine sub-bottom measurements which are not specifically designed as one-off large deployments.

Of course the assumptions in this model will limit its accuracy. Geological expertise will be required in each case to assess the likelihood that a layer is in fact horizontal, and that the perceived dipping is due to sound speed perturbations. In the model used here, the material parameters of the sediment enter only through the term c_s, and other than this and the material density there is no reflection of the complexity of propagation that can occur in such materials (see Section 1). However because the method relies on sound speed perturbations, it is not as sensitive to inclusion of some parameters as would be one based on absorption. Furthermore, whilst improved models for sound speed will be available for substitution into this scheme (and whilst the assumption of quasi-static dynamics can be replaced using a more sophisticated inversion routine), the importance of this report lies in expressing such a simple scheme for obtaining the void fraction and extent (in the vertical and horizontal) of bubble populations in marine sediment.

6 Appendix

This Appendix considers the effect of the violation of the assumption that, at a given horizontal coordinate, the bubble population (when averaged over lengthscales of the order of an acoustic wavelength) is uniform with depth throughout the measured profile. This assumption was employed throughout the body of this report, and yet it clearly will be violated in many practical scenarios.

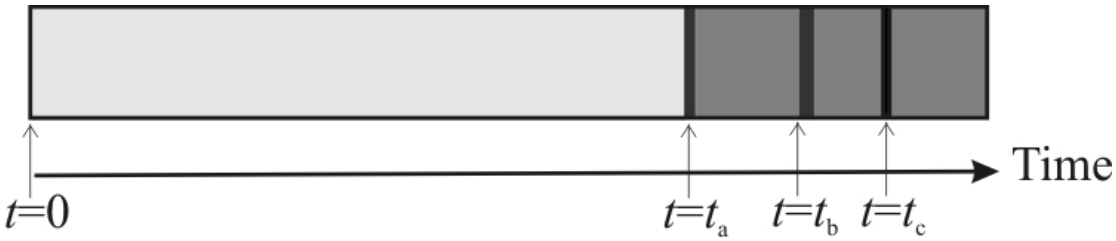

Figure 8. Greyscale schematic of the time history of the acoustic return from a layered gasless seabed. The echo which is received at time t_b occurs from a layer (termed 'b') which is at depth d_b below the seabed, and the echo which is received at time t_c occurs from a layer (termed 'c') which is at depth d_c below the seabed, in gas-less conditions.

Consider Figure 8, which add as extra layer to the schematic shown in Figure 4. In gas-less conditions, the two-way travel time to receive an echo from the top of the seabed (at depth d_w) is

$$t_a = 2d_w / c_w \qquad (25)$$

Similarly, in gas-less conditions, the two-way travel time to receive an echo from the top of the seabed (at depth d_w) a layer at depth d_b is

$$t_b = 2(d_w / c_w + d_b / c_s) \qquad (26)$$

and the two-way travel time to receive an echo from a layer at depth d_c is

$$t_c = 2(d_w / c_w + d_c / c_s) \qquad (27)$$

.

Using an algorithm which produces the sonar profile by assuming a constant sediment sound speed of c_s, then from equation (26) the depth of the layer d_b below the seabed is given by:

$$d_b = c_s(t_b / 2 - d_w / c_w) \quad (28)$$

The same algorithm would of course calculate the depth of the layer d_c below the seabed (equation (27)) as:

$$d_c = c_s(t_c / 2 - d_w / c_w) \quad (29)$$

.

However if the region between the top of the seabed and the layer at depth d_b contains gas such that the sound speed there is c_{eff} , then the two-way travel time to receive an echo from the top of the seabed (at depth d_w) a layer at depth d_b is

$$t_b^{'} = 2(d_w / c_w + d_b / c_{eff}) \quad (30)$$

and the two-way travel time to receive an echo from a layer at depth d_c is

$$t_c^{'} = 2(d_w / c_w + d_b / c_{eff} + (d_b - d_c) / c_s) \quad (31)$$

.

Consequently, if the algorithm which produces the sonar profile were to assume a constant sediment sound speed of c_s , then the perceived depth of layer 'b' ($d_b^{'}$) would be found by replacing t_b from (30) in equation (28) by $t_b^{'}$ to give:

$$d_b^{'} = c_s(t_b^{'} / 2 - d_w / c_w) = c_s(d_w / c_w + d_b / c_{eff} - d_w / c_w) = c_s d_b / c_{eff} \quad (32)$$

However the perceived depth of layer 'c' ($d_c^{'}$) would be found by replacing t_c from (31) in equation (29) by $t_c^{'}$ to give:

$$d_c^{'} = c_s(t_c^{'} / 2 - d_w / c_w) = c_s(d_w / c_w + d_b / c_{eff} + (d_b - d_c) / c_s - d_w / c_w) \quad (33)$$
$$= c_s(d_b / c_{eff} + (d_b - d_c) / c_s) = (d_b - d_c) + c_s d_b / c_{eff}$$

.

That is to say, that the depth of the layer is no longer increased by the same multiplicative factor c_s / c_{eff} as before (equation (23)). Rather, the depth interval between layers 'b' and 'c' is the same as it would be in the bubble-free condition, but layer 'c' has been translated downwards by the same absolute distance as was layer 'b'.

References

Anderson, A. L., and L. D. Hampton (1980a), Acoustics of gas-bearing sediment I. Background. *J. Acoust. Soc. Am., 67*(6), 1865-1889.

Anderson, A. L., and L. D. Hampton (1980b), Acoustics of gas-bearing sediment II. Measurements and models. *J. Acoust. Soc. Am., 67*(6), 1890-1905.

Anderson, A. L., F. Abegg, J. A. Hawkins, M. E. Duncan, and A. P. Lyons (1998), Bubble populations and acoustic interaction with the gassy floor of Eckernforde Bay, *Cont. Shelf Res., 18*(14-15), 1807-1838.

Andreassen, K., P.E. Hart and M. MacKay (1997), Amplitude versus offset modelling of the bottom simulating reflection associated with submarine gas hydrates, *Marine Geology, 137*(1-2), 25-40.

Biot, M. A. (1956a), Theory of Propagation of Elastic Waves in Fluid-Saturated Porous Solids: 1. Low-Frequency Range, *J. Acoust. Soc. Am., 28*(2), 168-178.

Biot, M. A. (1956b), The theory of propagation of elastic waves in a fluid-saturated porous solid: 2. Higher frequency range, *J. Acoust. Soc. Am., 28*(2), 179-191.

Biot, M.A. (1962), Generalized Theory of Acoustic propagation in porous dissipative media, *J. Acoust. Soc. Am., 34*(9), 1254-1264.

Boudreau, B. P., C. Algar, B. D. Johnson, I. Croudace, A. Reed, Y. Furukawa, K. M. Dorgan, P. A. Jumars, A. S. Grader and B. S. Gardiner, (2005), Bubble growth and rise in soft sediments. *Geology,* 33(6), 517-520.

Bull, J. M., M. Gutowski, J. K. Dix, T. J. Henstock, P. Hogarth, T. G. Leighton and P. R. White, (2005a) 3D chirp sub-bottom imaging system: design and first 3D volume. *Proceedings of the International Conference on Underwater Acoustic Measurements, Technologies and Results*, J.S. Papadakis and L. Bjorno, eds. (Crete, 2005) 777-782.

Bull, J. M., M. Gutowski, J. K. Dix, T. J. Henstock, P. Hogarth, T. G. Leighton and P. R. White, (2005b) Design of a 3D Chirp sub-bottom imaging system. *Mar. Geophys. Res.*, 26, 2005, 157-169.

Chapman, R. B., and M. S. Plesset, (1971), Thermal effects in the free oscillation of gas bubbles. *Trans ASME D: J Basic Eng., 93*, 373-376.

Domenico, S. N. (1976), Effect of brine-gas mixture on velocity in an unconsolidated sand reservoir, *Geophysics*, *41*(5), 882-894.

Domenico, S. N. (1977), Elastic properties of unconsolidated porous sand reservoirs, *Geophysics*, *42*(7), 1339-1368.

Fleischer, P., T. H. Orsi, M. D. Richardson, and A. L. Anderson (2001), Distribution of free gas in marine sediments: a global overview, *Geo-Marine Letters*, *21*, 103-122.

Foldy, L. L. (1945), The multiple scattering of waves, *Phys. Rev.*, *67*, 107-119.

Gregory, A. R. (1976), Fluid saturation effects on dynamic elastic properties of sedimentary rocks, *Geophysics*, *41*(5), 895-921.

Gutowski, M., Bull, J. K. Dix, T. J. Henstock, P. Hogarth, T. Hiller, T. G. Leighton and P. R. White, (2008), 3D High-Resolution Acoustic Imaging of the Sub-Seabed. *Applied Acoustics* (in press).

Hawkins, J.A., and A. Bedford (1992), Variational theory of bubbly media with a distribution of bubble sizes. 2. Porous solids, *Int. J. Engineering Science, 30*(9), 1177-1186.

Herskowitz, M., S. Levisky, and I. Shreiber (2000), Attenuation of ultrasound in porous media with dispersed microbubbles, *Ultrasonics*, *38*, 767-769.

Hill, J. M., J. P. Halka, R. Conkwright, K. Koczot, and S. Coleman (1992), Distribution and effects of shallow gas on bulk estuarine sediment properties, *Cont. Shelf Res., 12*(10), 1219-1229.

Judd, A. G. (2003), The global importance and context of methane escape from the seabed, *Geo-Marine Letters*, *23*, 147-154.

Judd A. G., and M. Hovland (1992), The evidence of shallow gas in marine sediments, *Cont. Shelf Res.*, *12*(10), 1081-1095.

Leighton, T. G. (1994), *The Acoustic Bubble*, Academic Press, London.

Leighton, T. G. (2004), From seas to surgeries, from babbling brooks to baby scans: The acoustics of gas bubbles in liquids, *Int. J. Modern Physics B, 18*(25), 3267-3314.

Leighton T G, Meers S D and White P R (2004), Propagation through nonlinear time-dependent bubble clouds, and the estimation of bubble populations from measured acoustic characteristics. *Proceedings of the Royal Society A*, **460**(2049), 2521-2550

Leighton T G, (2007a), Theory for acoustic propagation in marine sediment containing gas bubbles which may pulsate in a non-stationary nonlinear manner, *Geophysical Research Letters*, **34**, L17607, doi:10.1029/2007GL030803

Leighton T G. Theory for acoustic propagation in solid containing gas bubbles, with applications to marine sediment and tissue, *ISVR Technical Report No. 318* (2007b)

Leighton, T. G. (2007c), What is ultrasound?, *Progress in Biophysics and Molecular Biology*, *93*(1-3), 3-83.

Lenham, J. M., J. M. Bull and J. K. (1998), A marine geophysical survey of Strangford Lough. *Archaeology Ireland*, *11*, 18-20.

Minshull, T. A., S. C. Singh, and G. K. Westbrook (1994), Seismic velocity structure at a gas hydrate reflector, offshore western Colombia, from full waveform inversion, *J. Geophys. Res.*, *99*(B3), 4715-4734.

Phelps A D and Leighton T G (1998), Oceanic bubble population measurements using a buoy-deployed combination frequency technique. *IEEE Journal of Oceanic Engineering*, *23*(4), 400-410.

Ostrovsky L. A., S. N. Gurbatov and J. N. Didenkulov, (2005), Nonlinear acoustics in Nizhni Novgorod (A review) . Acoustical Physics, 51(2), 114-127.

Prosperetti, A. and Y. Hao (1999), Modelling of spherical gas bubble oscillations and sonoluminescence, *Phil. Trans. R. Soc. Lond. A*, *357*, 203-223.

Reed, A. H., B. P. Boudreau, C. Algar, and Y. Furukawa (2005), Morphology of gas bubbles in mud: A microcomputed tomographic evaluation, *Proc. 1st Int. Conf. Underwater Acoustic Measurements: Technologies and Results*, Heraklion, Crete (2005).

Richardson, M. D., and K. B. Briggs (1993), On the use of acoustic impedance values to determine sediment properties, *Proc. Institute of Acousics,* 15(2) pp. 15-23

Robb, G. B. N., T. G. Leighton, J. K. Dix, A. I. Best, V. F. Humphrey, and P. R. White (2006), Measuring bubble populations in gassy marine sediments: A review, *Proc. Inst. Acoust.*, *28*(1), 60-68.

Robb G B N, Leighton T G, Humphrey V F, Best A I, Dix J K and Klusek Z (2007a), Investigating acoustic propagation in gassy marine sediments using a bubbly gel mimic. *Proceedings of the Second International Conference on Underwater Acoustic Measurements, Technologies and Results,* J.S. Papadakis and L. Bjorno, eds. (Heraklion, Crete) 2007, 31-38.

Robb G B N, Leighton T G, Humphrey V F, Best A I, Dix J K and Klusek Z (2007b), *Investigating acoustic propagation in gassy marine sediments using a bubbly gel mimic, ISVR Technical Report* 315, University of Southampton.

Sills, G. C., S. J. Wheeler, S. D. Thomas, and T. N. Gardiner (1991), Behaviour of offshore soils containing gas bubbles, *Geotechnique*, *41*(2), 227-241.

Smeulders, D. M. J., and M. E. H. Van Dongen (1997), Wave propagation in porous media containing a dilute gas-liquid mixture: theory and experiments, *J. Fluid Mech.*, *343*, 351-373.

Stoll, R. D. (1974), *Sediment Acoustics, Lecture Notes in Earth Science 26*, Springer-Verlag, New York.

Stoll, R. D., and E. O. Buatista (1998), Using the Biot theory to establish a baseline geoacoustic model for seafloor sediments, *Continental Shelf Res.*, *18*, 1839-1857.

Vorkurka, K. (1986), Comparison of Rayleigh's, Herring's, and Gilmore's models of gas bubbles, *Acustica*, *59*, 214–219.

Wilkens, R. H. and M. D. Richardson (1998), The influence of gas bubbles on sediment acoustic properties: in situ, laboratory, and theoretical results from Eckernförde Bay, Baltic sea. Continental Shelf Research, 18(14-15), 1859-1892.

Wheeler, S. J., and T. N. Gardiner (1989), Elastic moduli of soils containing large gas bubbles, *Geotechnique*, *39*(2), 333-342.